2020 EAGE ANNUAL
82ND CONFERENCE + EXHIBITION
AMSTERDAM | THE NETHERLANDS
NOW IN WINTER
8-11 DECEMBER

Th_P06_03

Applicability of Characterizing Fracture Apertures with Flow-Elastic Relations

J.H.Y. Ma[1]*, Y.E. Li[1], A. Cheng[1]

[1] National University of Singapore

Summary

Understanding of flow-elastic relations help to characterize rock properties and predict their variations under pressure changes due to the implicit linkage between two aspect of properties through geometries. In this study, we have investigated the relations based on single rough fractures. By a parametrization description of fracture apertures with statistical parameters of spatial correlation and global variation, we have synthesized fracture apertures resulting in various types of relative surface roughness. Numerical simulations have been conducted to estimate for the effective permeability, transport characteristics and P-wave velocities of these fractured rocks. We have addressed on the stress sensitivity of roughness parameters on the joint fracture properties, and whether these flow-elastic relations could be used to resolve for the statistical roughness parameters.

Introduction

Distribution of open apertures and closed contacts in fractures are the fundamental properties controlling their response towards fluid flow and elastic properties. While the opening size and connectivity of apertures contributes to the flow conductance, the asperity compression at closed area and open volumes provides characteristics of elastic wave responses in the host rocks. Therefore, flow and elastic properties in fractures could be linked implicitly through the knowledge of fracture aperture distribution (Pyrak-Nolte & Morris, 2000). While the elastic properties in rocks are often measured with wave velocities, flow properties are conventionally represented by the permeability of fluids which is a macroscopic measure of the flow capability of medium. Nevertheless, the transient flow properties are shown to be indicative on the heterogeneity of medium

Subsequently, Ma *et al.* (2019) have illustrated that fracture with different roughness distributions exhibits distinctive changes in macroscopic and transient flow properties when subjected to compressions. With further understanding of the aperture dependency on flow and elastic properties in fractures, we could construct the flow-elastic relations for various fracture aperture distributions. From which, we may investigate how the roughness parameters control the flow-elastic characteristics, and whether it is possible to differentiate for fracture aperture distribution with the appropriate flow-elastic relation(s).

Methodology

We consider a cubic volume of rock of lengths L=100m which host a horizontal-oriented single rough fracture. The first-contact aperture height variations are parametrized with two roughness parameters: 1) spatial autocorrelation lengths (λ); and 2) root-mean-squared relative surface roughness (σ). Assuming the size of fracture apertures follows a log-normal distribution, we synthesize, in frequency domain, the random aperture maps $h(x,y)$ in digital resolution of 128 × 128 pixels (Ruan & McLaughin, 1998), by considering the spatial isotropic λ between $L/64$ to $L/16$ and σ between $L/1500$ to $L/900$. A non-interactive rock asperity assumption is used when modelling fracture compression. Thus, the aperture change is linear with fracture compression displacement, with a zero minimum which denotes fracture surfaces are at contact.

Figure 1 shows examples of synthesized fractures of different roughness parameters, all with the mean aperture height of 0.1m. Comparing figure 1(a) and 1(b), longer λ signifies less spatially varying aperture height, thus leading to larger area of contacts as well as openings. The overall aperture size distribution is the same. Comparing figure 1(a) and 1(c), higher σ indicates large apertures, and more contacts with same mean aperture.

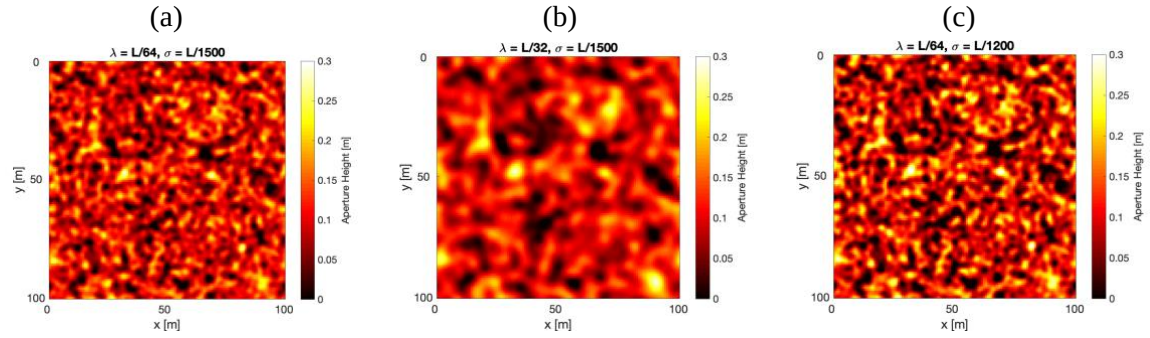

Figure 1 *Examples of synthesized aperture with (a) λ=L/64, σ=L/1500; (b) λ=L/64, σ=L/1200; and (c) λ=L/64, σ=L/1200 respectively.*

We considered both the macroscopic and the transient flow properties of the fractures. The macroscopic flow property is measured by the effective permeability. With a constant applied hydraulic pressure on a lateral pair of boundaries, and the other boundaries as impermeable in the water-saturated fracture, we modelled the depth-averaged flow velocities with Darcy's law where the local permeability is related to $h_2/12$. Effective permeability is evaluated with the outgoing flow flux.

The transient flow characteristics in fracture compression could be revealed with the transportation time variations among fluid particles. With a uniform injection of particle along high fluid pressure boundary under the simulated steady-state flow background, the transportation path and

nodal residence time are simulated with a spatial Markov model (Kang *et al.*, 2011). The probability of particle breakthrough falls log-linear with time for slow transported particles. We account for the fracture transient flow property with the log-breakthrough tail slope.

The effective moduli of the fracture hosting rock are evaluated with the Hudson-Cheng's model (Cheng 1993), which corrects for crack-induced compliance to the moduli of isotropic intact rocks. Translating into the context of equivalent ellipsoidal cracks, aspect ratio is substituted with square root of the ratio between the variance of aperture heights and the open area in fracture. Young's modulus of 70 GPa and Poisson's ratio of 0.25 and density of 2650 kg/m3 are assumed for the intact rocks. The velocity of transmitted *P*-wave across rough fracture hosting rock could be estimated as the square root between the effective moduli C_{33}^{*} and overall density of the fluid-filled fractured rock. The corresponding effective stress applied on fracture under any given compression displacement are estimated with a linear elastic model based on the fracture contract area and compressed displacement of background asperities (Unger & Mase, 1993).

With a mean aperture height of 0.1m set as the reference compression state of the rough fractures, we have simulated for the effective permeability, log-breakthrough tail slope, *P*-wave velocities and the effective stress on fracture with the incremental fracture compression displacement of 0.01m. 50 simulation realizations are made for each set of roughness parameters and the results are represented with their averages. The flow-elastic relations are illustrating by cross plotting the effective permeability and log-breakthrough tail slope against the *P*-wave velocities respectively.

Results and Discussions

Figure 2(a) shows the simulated stress-dependent relations between effective permeability and *P* velocities of all simulated fracture roughness parameters. The differences in permeability-velocity correspondence are not apparent at low compressions. Under higher effective stress conditions, where permeability is low and velocities are high, distinctive relations between effective permeability and *P*-wave velocities are observed. Figure 2(b) show the simulated relations between tail slope of log-breakthrough curve and elastic wave velocities respectively. It is shown that the relations are distinctive and exists for a larger range of effective stress. The more distinctve transient flow-elastic relations under lower stress suggest that it would provide supplementary information for characterization in addition to effective permeability.

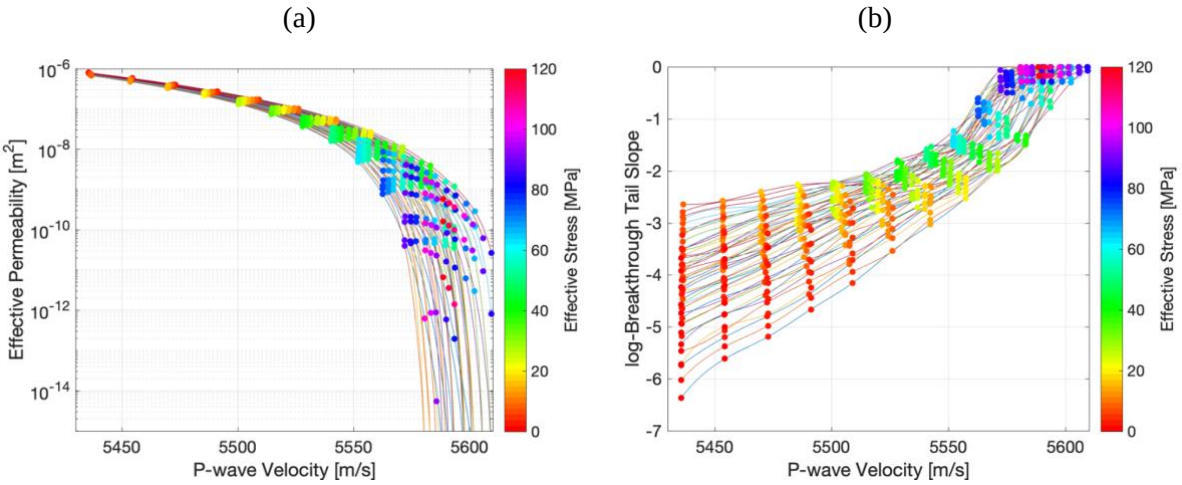

Figure 2 *The simulated stress-dependent relations between (a) effective permeability; and (b) log-breakthrough tail slope and P-wave velocity respectively for all fracture roughness parameters.*

The stress sensitivity of the macroscopic and transient flow-elastic relations are shown in Figure 3(a) and (b) respectively. The permeability-velocity ratio could vary substantially under high stress. The difference among ratios between log-breakthrough tail slope and velocities remains fairly distinct across all range of effective. The stress sensitivity of these ratio provides an indication for the applicable range for aperture characterization of the flow-elastic relations.

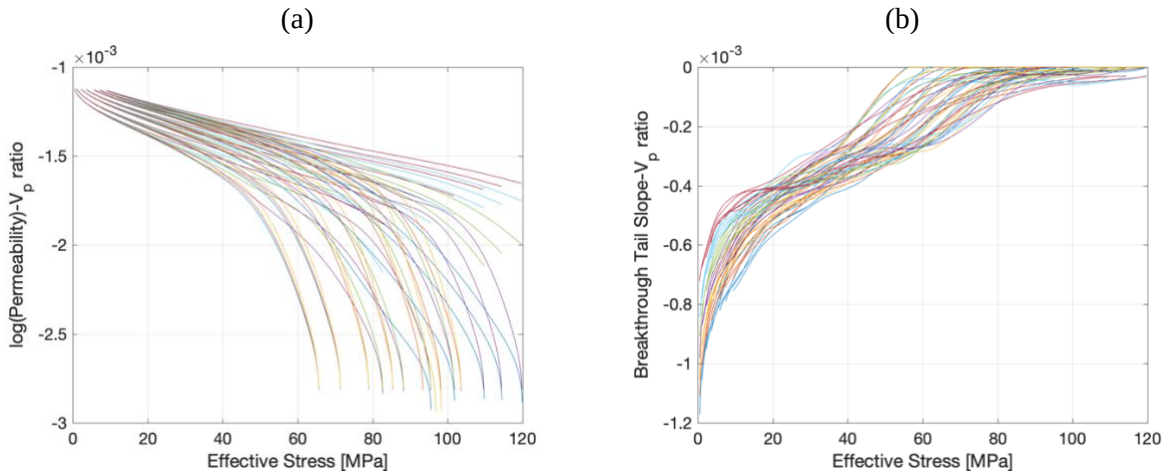

Figure 3 *The stress dependency of (a) effective permeability-P wave velocities; and (b) log-breakthrough tail slope-P-wave velocity relations for all fracture roughness parameters.*

Figure 4(b) and (c) compares the permeability-velocity profiles of fractures with same λ length and same σ respectively. The profiles for both cases show distinction under high effective stress, although for different reasons. The effective permeability of fractures is a collective effect of both the λ and σ, while *P*-wave velocity depends only on the σ only as λ has no effect on the total contact or openings. For fractures with same λ but different σ, the variations in relation profiles are due to larger differences in velocities compared to permeability as subjected to higher effective stress. The relations begin to appear distinctive above effective stress of 40 MPa. For fractures with same σ but different λ, the variations are resulted from the permeability differences caused by difference in residual flow path connectivity, with similar total contact, thus also similar *P*-wave velocities.

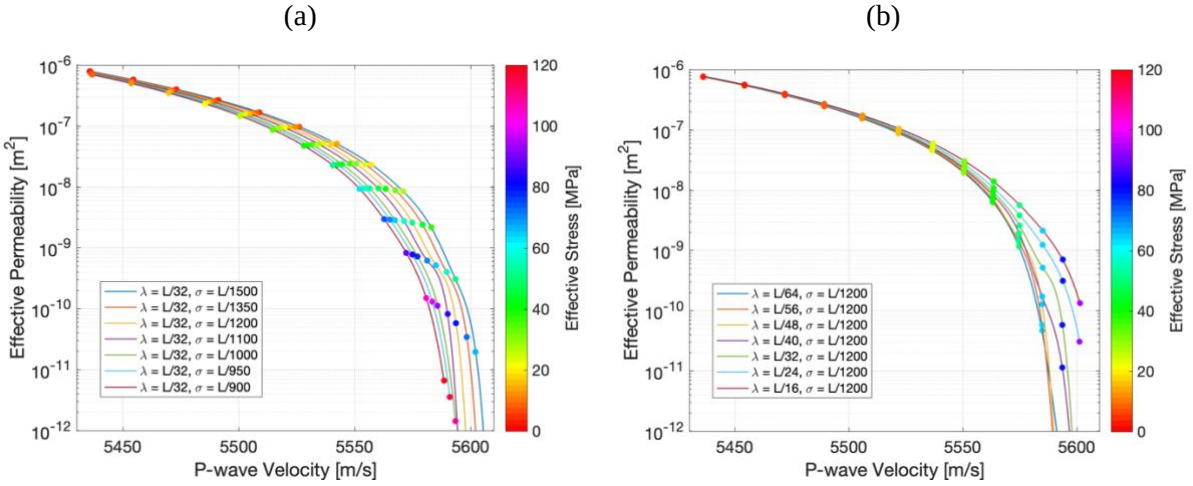

Figure 4 *The simulated relation between effective permeability and P-wave velocity for fractures with (a) λ=L/32*; and (b) *σ=L/1200*.

Figure 5(a) and (b) compares the transport-velocity profiles of fractures with same autocorrelation length and same relative surface roughness respectively. Fractures with same autocorrelation length shows mostly the systematic distinction for different relative surface roughness, as the characteristics of transports are heavily aperture connectively driven. Differences in aperture height with same conduit path affects the individual travel time but little on population statistics. However, for fractures with different σ, the tail slope of log-breakthrough curves changes differently with velocities for various λ. This is because compressions have created different available pathways in these fractures. Besides, the relations converge under high compressions, indicating the lost of differentiating power for λ under these circumstance. The genesis of preferential flow paths under high effective stress on fractures has caused transport time to increase exponentially. Though this

makes the relation between tail slope and velocity for different λ to collapse for effective stress above 50 MPa, distinctive characteristics still exist for different σ.

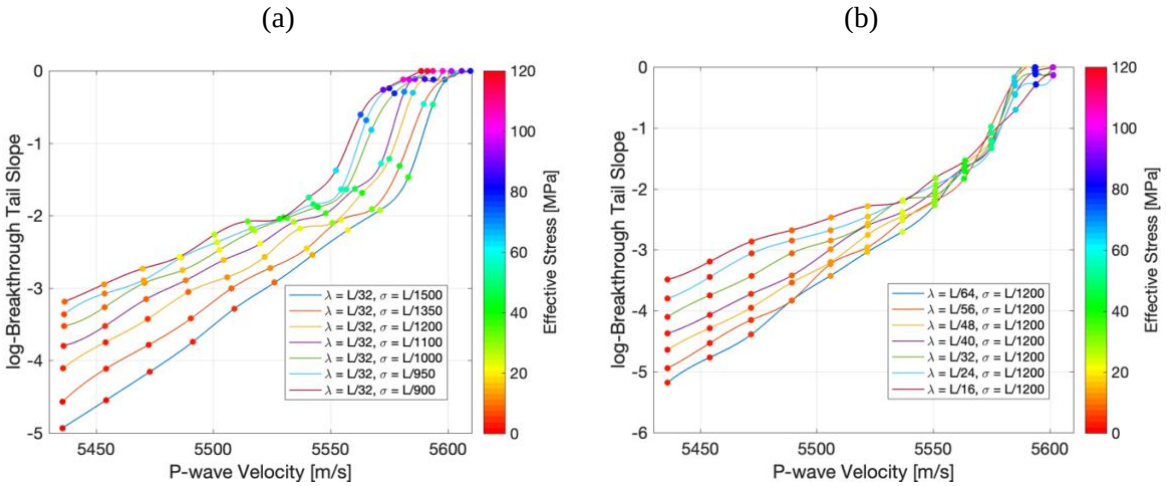

Figure 5 *The simulated relation between log-breakthrough tail slope and P-wave velocity for fractures with (a) λ=L/32*; and (b) *σ=L/1200*.

Conclusions

In this study, the stress-dependent flow-elastic properties of single rough fracture hosting rocks are being simulated, with the roughness-induced aperture variation parameterized using the first-contact autocorrelation length and relative surface roughness. The relations among effective permeability, transport characteristics and *P*-wave velocities are established. The relative sensitivity of each roughness parameters on the joint properties are examined, to reveal the differentiating power of the respective flow-elastic relations on fracture aperture characterizations.

The relations between effective permeability and *P*-wave velocities are suggested possible for distinguishing both statistical fracture roughness parameters, when effective stress is higher than 40 MPa. Nevertheless, the relations between transport characteristics and *P*-wave velocities are shown to be suitably adoptable differentiating for both roughness parameters when effective stress is beneath 50 MPa. These observations have provided confidence the combination of effective permeability-velocity and transient flow-velocity relations could be applied for fracture characterization purposes.

Acknowledgements

The authors acknowledge the financial support of Petroleum Engineering Professorship from Singapore Economic Development Board. Dr. Elita Li is also funded by Ministry of Education Tier-1 Grants: R-302-000-182-114 and R-302-000-196-592.

References

Cheng, C. H. [1993]. Crack models for a transversely isotropic medium. *Journal of Geophysical Research: Solid Earth*, **98**(B1), 675-684.

Kang, P. K., Dentz, M., Le Borgne, T., and Juanes, R. [2011]. Spatial Markov model of anomalous transport through random lattice networks. *Physical review letters*, **107**(18), 180602.

Ma, J.H.Y., Li, Y.E., and Cheng, A. [2019]. Dependency of flow and transport properties on aperture distributions and compression states. *Geophysical Prospecting*, **67**(4), 900-912.

Pyrak-Nolte, L. J., and Morris, J. P. [2000]. Single fractures under normal stress: The relation between fracture specific stiffness and fluid flow. *International Journal of Rock Mechanics and Mining Sciences*, **37**(1-2), 245-262.

Unger, A. J. A., and Mase, C. W. [1993]. Numerical study of the hydromechanical behavior of two rough fracture surfaces in contact. *Water Resources Research*, **29**(7), 2101-2114.